32nd Annual International Conference of the IEEE EMBS
Buenos Aires, Argentina, August 31 - September 4, 2010

Denoising of LSFCM images with compensation for the *Photoblinking/Photobleaching* effects

Isabel Rodrigues and J. Miguel Sanches

***Abstract*— Fluorescence confocal microscopy images present a low *signal to noise ratio* and a time intensity decay due to the so called *photoblinking* and *photobleaching* effects. These effects, together with the Poisson multiplicative noise that corrupts the images, make long time biological observation processes very difficult.**

In this paper a Bayesian denoising algorithm for Poisson data is presented where two different *a priori* distributions, one in the time domain and the other in the space domain, are used together to regularize the solution. These distributions, used to describe the spatio-temporal correlation among neighboring pixels, along the time, allow to greatly improve the SNR of the denoised solution, mainly, in the last images on the sequence that present worst SNR.

In the observation model the *photoblinking* and *photobleaching* effects are explicitly taken into account where the theoretical foundations for the corresponding intensity decay model, outlined here, were recently proposed by the authors.

Monte Carlo experiments and validation with other models, using synthetic data, are presented to characterize the performance of the algorithm. Also an example with a real data sequence is included to illustrate its application.

***Index Terms*— Photobleaching, Poisson Denoising, convex, Bayesian, Total Variation, Log-Euclidean Potentials.**

I. Introduction

Fluorescence microscopy imaging became a common tool in biomedical research since it allows the study of the dynamics of living cells in an almost non-invasive manner.

The phenomenon of fluorescence consists on the emission of light with a longer wavelength than the one of the incident radiation, by excited molecules within nanoseconds after the absorption of photons. The fluorophore is the component of the molecule responsible for its capability to fluoresce.

The *photoblinking/photobleaching* (PBPB) effects lead to an intensity fading of a fluorescent probe along the time. This effect is caused by quantum phenomena associated with the electronic excitation and photochemical reactions among the fluorescent and the surrounding molecules induced by the incident radiation that temporarily or irreversibly destroy their ability to fluoresce. Since illumination is needed to excite and observe the tagging fluorescent proteins in the specimen and all the fluorophores will eventually photobleach upon extended excitation, the acquisition of this type of images becomes a hard task for long exposures. The reduction of the intensity of the incident radiation can attenuate this effect but leads to a decreasing in the *signal to noise ratio* (SNR) of the acquired images. Due to the small amount of detected radiation and to the huge optical and electronic amplification needed in the experiments, the resulting images are corrupted with a severe type of multiplicative noise typically described by a Poisson distribution.

In this paper a denoising algorithm for Poisson data that explicitly takes into account the global PBPB effects is presented. The goal is to estimate the non-constant basic nucleus morphology and the rates of intensity decay due to PBPB, from laser scanning fluorescence confocal microscope (LSFCM) images of cells.

Different types of PBPB image intensity decay laws are considered in the literature [1] being the most common the single and multi decaying exponentials. Here the global intensity decrease along the time is modeled by using a weighted sum of two negative exponentials with constant rates. Theoretical foundations for this model, outlined in section II, were described in [2] for the first time.

The algorithm is formulated in the Bayesian framework as an optimization task where a convex energy function is minimized by using the *maximum a posteriori* (MAP) criterion and a Poisson data fidelity term.

The local Markovianity of the cell morphology to be estimated is a reasonable assumption that leads to a Gibbs *a prior* distribution where suitable potential functions should be considered. Quadratic potentials are extensively used, but they produce over-smoothed solutions. *Edge preserving priors* including non quadratic potentials such as *total variation* (TV) have been successfully applied to several image denoising problems. Very recently a new type of potential functions was proposed in [3]. This approach, based on log-Euclidean norms, is suitable to be used here due to the positiveness nature of the unknowns to be estimated and to the mathematical easiness it introduces in the resulting objective function.

This work is a novel evolution of previous work published by the authors [4] where a new PBPB model, presented in [2], is explicitly included in the observation model.

In section II a brief description of the adopted *photoblinking/photobleaching* model is presented and in section III the denoising problem is formulated. In section IV the performance of the algorithm is evaluated by means of a Monte Carlo experiment carried on generated synthetic data with a low SNR (4dB-12dB). Also a validation of the proposed model with other state-of-the-art models is presented. Real data of a *HeLa* immortal cell [5] nucleus, acquired

This work was supported by project the FCT (ISR/IST plurianual funding) through the PIDDAC Program funds.

Isabel Rodrigues (irodrigues@deetc.isel.ipl.pt) is with Institute for Systems and Robotics and with Instituto Superior de Engenharia de Lisboa

J. Miguel Sanches (jmrs@ist.utl.pt) is with Institute for Systems and Robotics at the Instituto Superior Técnico, 1049-001 Lisbon, Portugal.

in a laser scanning fluorescence confocal microscope, are used to illustrate the application of the algorithm. Section V concludes the paper.

II. *Photoblinking/Photobleaching* Model

In an LSFCM images sequence, the intensity at each pixel is related with the non-uniform distribution of the *fluorescent protein* molecules across the cell nucleus. However, the fading effect observed in these image sequences due to the *photoblinking* and *photobleaching* phenomena, related with a temporarily or permanently loose ability of the fluorophores to fluoresce, may be modeled in a global basis without considering local variations due to transport or diffusion processes occurring inside the cell.

It is assumed that the fluorescent molecules can be in three main states: active *ON-state*, active *OFF-state* and inactive *BLEACHED-state* [6]. When they are at the *ON-state* they are able to fluoresce and be observed. In the active *OFF-state* they are not emitting fluorescent radiation and therefore they are not visible although they are able to recover and fluoresce again. Finally in the inactive *BLEACHED-state* they become permanently unable to fluoresce. A model describing the dynamics associated with the transitions among these states was proposed in [2]. In the model, the number of molecules at the *ON-state*, that is proportional to the mean intensity of the image at the instant t, $\overline{y}(t) \propto n_{ON}$, can be described by the following second order differential equation

$$\frac{d^2 n_{ON}}{dt^2} + (\upsilon + \xi(I))\frac{dn_{ON}}{dt} + \beta_{ON}\xi(I) n_{ON} = 0 \qquad (1)$$

where υ, ξ, υ and β_{ON} are parameter associated with the concentrations and state transition dynamics of the molecules within the cell and I is the amount of incident radiation.

The solution to this equation is

$$n_{ON}(t) = \gamma_1 e^{-\lambda_1 t} + \gamma_2 e^{-\lambda_2 t}, \quad t \geq 0 \qquad (2)$$

where γ_1 and γ_2 are constants computed using the initial conditions. Given the physical constraints of the problem it can be proved that λ_1 and λ_2 are always positive real constants [2]. This result is in accordance with most used model in the literature obtained from experimental evidences. Here, however, the two decaying exponentials model describing the PBPB effects is based on the physical quantum process involved.

III. Problem Formulation

Each fluorescence microscopy sequence of images is denoted by a 3D tensor, $\mathbf{Y} = \{y_{i,j,t}\}$, with $0 \leq i,j,t \leq N-1, M-1, L-1$, where each data point, $y_{i,j,t}$, is corrupted with Poisson noise with parameter $x_{i,j,t}$ that decrease along the time due to the PBPB effects according to (2). Therefore, each point of the noiseless cell nucleus images, $\mathbf{X}$, can be written as $x_{i,j,t} = f_{i,j,t} n_{ON}(t)$, where $\mathbf{F} = \{f_{i,j,t}\}$ stands for the *time varying* underlying morphology of the cell nucleus, γ_1, γ_2, λ_1 and λ_2 in $n_{ON}(t)$ are constants to be estimated by fitting (2) to the mean of the noisy images along the time $\overline{y}(t)$.

Let us denote by $\mathbf{\Theta}$ the set of estimated parameters $\{\hat{\lambda_1}, \hat{\lambda_2}, \hat{\gamma_1}\hat{\gamma_2}\}$. The ultimate goal of the proposed algorithm is to estimate the cell nucleus underlying morphology, $\mathbf{F}$, from these noisy data, $\mathbf{Y}$, exhibiting a low SNR. The Bayesian approach using the MAP criterion is adopted to estimate $\mathbf{F}$. This problem may be formulated as the energy optimization task $(\hat{\mathbf{F}}) = \arg\min_{\mathbf{F}} E(\mathbf{F}, \mathbf{\Theta}, \mathbf{Y})$, where the energy function $E(\mathbf{F}, \mathbf{\Theta}, \mathbf{Y}) = E_Y(\mathbf{F}, \mathbf{\Theta}, \mathbf{Y}) + E_F(\mathbf{F})$ is a sum of two terms, $E_Y(\mathbf{F}, \mathbf{\Theta}, \mathbf{Y}) = -\log(p(\mathbf{Y}, \mathbf{F}|\mathbf{\Theta}))$, called *data fidelity term*, and $E_F(\mathbf{F}) = -\log(p(\mathbf{F}))$, called *a prior* term. The *a prior* information on $\mathbf{\Theta}$ is merely its overall constancy.

Assuming the independence of the observations, and a Poisson model for the noise, the *data fidelity term*, is

$$\begin{aligned} E_Y(\mathbf{F}, \mathbf{\Theta}, \mathbf{Y}) &= \sum_{i,j,t} [f_{i,j,t}\hat{n}_{ON}(t) - y_{i,j,t} \log(f_{i,j,t}\hat{n}_{ON}(t))] \\ &+ K \end{aligned} \qquad (3)$$

where K is a constant and $\hat{n}_{ON}(t)$ is given by (2).

By assuming $\mathbf{F}$ as a *Markov Random Field* (MRF), $p(\mathbf{F})$ can be written as a Gibbs distribution,

$$p(\mathbf{F}) = \frac{1}{T}\exp[-\sum_{c \in C} V_c(\mathbf{F})],$$

where T is the normalizing constant and $V_c(.)$ are the potential functions. The selection of the most convenient potential functions to each problem is crucial since they act upon the solution. In this paper *log-Euclidean* [3] based potential functions are used,

$$V_c = \sqrt{\log^2(\frac{f}{f_a}) + \log^2(\frac{f}{f_b})} \qquad (4)$$

where f_a and f_b are neighbors of f in a second order clique (see Fig.1). These functions, that can be interpreted as *log-total variation* potentials, produce edge-preserving *a priori* terms which are suitable to keep the details of the cell nucleus morphology and simultaneously to remove the noise in the homogeneous regions. Therefore, the *a prior* term is

$$\begin{aligned} E_F(\mathbf{F}) &= \alpha \sum_{i,j,t} \sqrt{\log^2(\frac{f_{i,j,t}}{f_{i-1,j,t}}) + \log^2(\frac{f_{i,j,t}}{f_{i,j-1,t}})} \\ &+ \beta \sum_{i,j,t} \sqrt{\log^2(\frac{f_{i,j,t}}{f_{i,j,t-1}})} \end{aligned} \qquad (5)$$

where α and β are strictly positive hand tunning parameters to reduce or increase the strength of the regularization in the space and time dimensions respectively. This *anisotropic filtering* approach, where different regularization parameters (or even different potential functions) are used in time and space, is described in detail in [7].

The formulated optimization problem is non-convex. However, performing the change of variable, $z_{i,j,t} = log(f_{i,j,t})$, it is possible to turn it into convex. The minimizers of $E(\mathbf{F}, \mathbf{\Theta}, \mathbf{Y})$ in $\mathbf{F}$ and of $E(\mathbf{Z}, \mathbf{\Theta}, \mathbf{Y})$ in $\mathbf{Z}$ are related by $\mathbf{Z}^* = \log(\mathbf{F}^*)$ due to the monotonicity of the logarithmic

function. The new convex objective function for this model is

$$E(\mathbf{Z},\boldsymbol{\Theta},\mathbf{Y}) = \sum_{i,j,t}[e^{z_{i,j,t}}\hat{n}_{ON}(t) - y_{i,j,t}z_{i,j,t} - y_{i,j,t}\log(\hat{n}_{ON}(t))] + \alpha\sum_{i,j,t}\sqrt{(z_{i,j,t}-z_{i-1,j,t})^2+(z_{i,j,t}-z_{i,j-1,t})^2} + \beta\sum_{i,j,t}\sqrt{(z_{i,j,t}-z_{i,j,t-1})^2} \quad (6)$$

The minimization of (6), accomplished by finding its stationary point in a point-wise basis, is performed by using the *iterative reweighed least squares* (IRWLS) method [8]. The final solution is obtained from $\hat{Z}$ by reversing the change of the variable, $\hat{\mathbf{F}} = e^{\hat{\mathbf{Z}}}$.

The convergence analysis of this method is long and out of the scope of this paper. Nevertheless a detailed convergence proof for a related algorithm is given in [8]. However, a relative error *per* iteration curve is presented in section IV illustrating the convergence ability of the proposed algorithm.

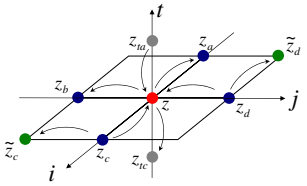

Fig. 1. Neighboring system, $\mathcal{S}$, involving the spatial and temporal neighbors.

IV. Experimental Results

In this section, results using synthetic and real data are presented. The synthetic data are used to characterize the performance of the denoising algorithm. A real images sequence is employed to illustrate the application of the algorithm to estimate the underlying morphology of a HeLa cell nucleus.

A. Synthetic Data

Results of a Monte Carlo (MC) experiment in 500 runs with 300 iterations each are presented in order to access the performance of the proposed algorithm. A moving pyramidal shape, $64\times64\times64$ pixels, synthetic morphology, was generated and an exponential decay term, $n_{ON}(t)$, $t=(0,...,63)$, with rates $\lambda_1 = 0.04$ image^{-1} and $\lambda_2 = 0.0025$ image^{-1}, was applied upon it to simulate the global PBPB effects. The sequence was then corrupted with Poisson noise in each run. The α and β regularization parameters were manually tunned. The mean square error (MSE) and the SNR of the estimated morphology were computed for each image and run. The averages of the referred quality metrics computed over the 500 runs of the MC experiment, are displayed in Fig. 2 a) and b), where the dotted and the solid lines stand respectively for the situations before and after applying the denoising algorithm. The plot in Fig. 2 a) shows an SNR improvement of the morphology images between $10dB$ and $15dB$. Also the MSE corroborates the assertions on the quality of the proposed denoising algorithm. Fig. 3 shows denoising results for the morphology corresponding to image

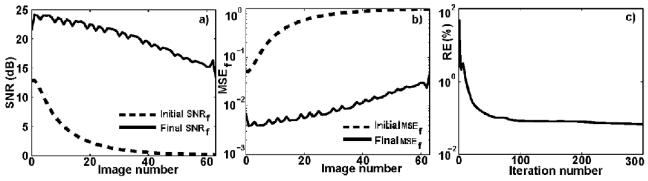

Fig. 2. Results of the Monte Carlo experiment for the morphology: (a) and (b) SNR curves and MSE curves for the morphology, before and after applying the proposed algorithm. (c) relative error based metrics (RE) *per* iteration, for the proposed algorithm.

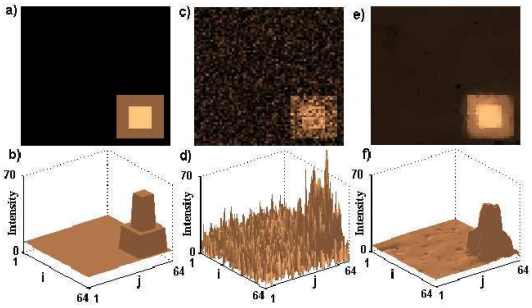

Fig. 3. Image 62 of the sequence of synthetic data: a) and b) true, c) and d) noisy, e) and f) estimated morphologies and respective surface representations.

62 of the synthetic sequence. It is notorious the ability of the algorithm to recover the degraded information in the noisy image. The profile plots in Fig. 4, taken along the diagonal of the image, correspond to the morphologies in images 2 and 62 of the synthetic sequence and show the ability of this denoising methodology to preserve the edges of the morphology. A relative error based measure (RE) was computed in

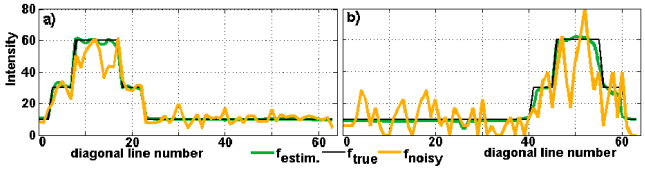

Fig. 4. Morphology profile plots corresponding to images 2-a) and 62-b) of the synthetic sequence (black lines - true, dark yellow lines - noisy, green lines - denoised). Green and black lines are hard to distinguish because the algorithm almost recovers the true images.

each iterative step as $RE = \frac{\|z^{(k)}-z^{(k-1)}\|}{\|z^{(k)}\|}$, its average was calculated over the 500 runs of the MC experiment and the plot is shown in Fig. 2 c) to illustrate the convergence ability of the algorithm. The proposed algorithm, denoted by LTV-LTV, was compared to Non-Local Means (NLM) algorithm [9], to a platelets (PLAT) and to a translation invariant Haar wavelet (TI-Haar) methodologies conceived for Poisson denoising [10]. The synthetic sequence was processed with the proposed LTV-LTV and with the other three algorithms. The SNR is used to evaluate the denoising results presented in Fig. 5. It is noticeable in these plots the good performance of the proposed LTV-LTV algorithm in what concerns the SNR quality metrics. The SNR curve presents higher values than the other algorithms, although PLAT also performs very good. The CPU time is also an important feature to take into account when selecting a denoising algorithm.The CPU time

to process the whole sequence with PLAT, NLM, LTV-LTV and TI-Haar was respectively 1319.2 s, 147.9 s, 17.2 s and 2.2 s, which means that the proposed algorithm is fast.

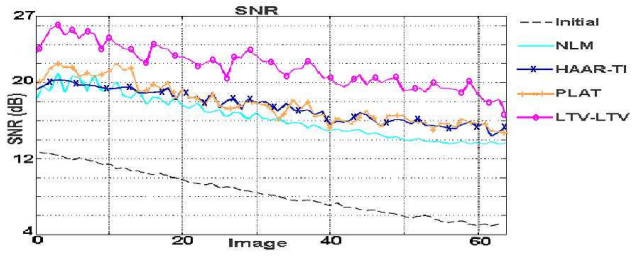

Fig. 5. Model Validation SNR results.

B. Real Data

The real data sequence used to show the application of the proposed algorithm consists of 100 LSFCM images of a HeLa cell nucleus acquired at a rate of 23.1 s using very low intensity light. The results of applying the presented denoising procedure are shown in Fig. 6 where a), b) stand for images 1 and 60 of the real sequence, c) and d) show the corresponding estimated underlying morphologies and e) and f) the respective profile plots along the diagonal of the images. Image 60 makes clear how difficult is to identify any details in the nucleus morphology. It is noticeable that this denoising methodology allows the recovery of the underlying morphology of a cell nucleus with a very low SNR.

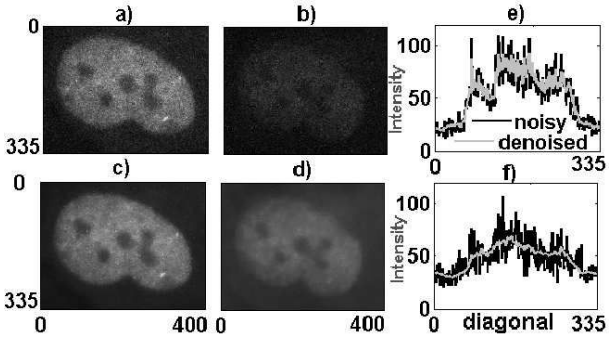

Fig. 6. HeLa cell nucleus. Sampling rate: 23.1s. Scale: $0.03\mu m/$pixel. a) and (b) Noisy images 1 and 30. (c) and (d) respective estimated underlying morphology, e) and f) respective noisy (black) and estimated (gray) morphology profiles. Data provided by the Molecular Medicine Institute of Lisbon, Portugal.

V. Concluding Remarks

In this paper a 2D+time denoising algorithm for LSFCM imaging is proposed. In this modality the images are corrupted with a type multiplicative noise assumed to follow a Poisson distribution. Furthermore, the global intensity of the images decreases along the time due to temporally (*photoblinking*) or permanently (*photobleaching*), ability loss of the fluorophore to fluoresce caused by quantum phenomena and photochemical reactions induced by the incident light. The global decreasing of the image intensity leads to a decreasing of the *signal to noise ratio* of the images, making the biological information recovery a difficult task. In the proposed algorithm this effect is explicitly taken into account and modeled by using a *two decaying exponential* function. Theoretical foundations for the use of this model are outlined.

The proposed approach is conceived as an optimization task with the *maximum a posteriori* (MAP) criterion where $log - Euclidean$ potential functions are used in the regularization terms. The energy function is designed to be convex and its minimizer is computed by using the Newton's algorithm and an iterative *reweighed least squares* based strategy to estimate the morphology of a cell nucleus.

A Monte Carlo experiment with synthetic data is used to assess the performance of the algorithm. This experiment shows the ability of the algorithm to strongly reduce the Poisson noise and to estimate the underlying morphology. The main characteristic of the algorithm is its ability to used all the information, even the last images of the sequence with a very low SNR, to recover the cell nucleus morphology. Validation with other models shows the good performance of the proposed algorithm.

Results of applying the proposed algorithm to a real data sequence show its effectiveness to cope with this type of noise and low SNR. Its performance is related to the use of edge preserving *a prior* distribution to model the statistical behavior of the cell morphology and to the use of an explicit *photobleaching* model.

References

[1] N. B. Vicente, J. E. D. Zamboni, J. F. Adur, E. V. Paravani, and V. H. Casco, "Photobleaching correction in fluorescence microscopy images," *Journal of Physics: Conference Series*, vol. 90, no. 012068, pp. 1 – 8, 2007.

[2] I. Rodrigues and J. Sanches, "Photoblinking/photobleaching differential equation model for intensity decay of fluorescence microscopy images," *IEEE International Symposium on Biomedical Imaging (ISBI10)*, 14-17 April 2010.

[3] Vincent Arsigny, Pierre Fillard, Xavier Pennec, and Nicholas Ayache, "Log-Euclidean metrics for fast and simple calculus on diffusion tensors," *Magnetic Resonance in Medicine*, vol. 56, no. 2, pp. 411–421, August 2006.

[4] I. Rodrigues and J. Sanches, "Fluorescence microscopy imaging denoising with log-euclidean priors and photobleaching compensation," in *Proceedings of IEEE International Conference on Image Processing (ICIP 2009)*, Cairo, Egypt, 2009.

[5] D.A. Jackson, F.J. Iborra, E.M. Manders, and P.R. Cook., "Numbers and organization of rna polymerases, nascent transcripts, and transcription units in hela nuclei.," *Mol Biol Cell*, vol. 9, pp. 1523–1536, 1998.

[6] Jörg Schuster, Jörg Brabandt, and Christian von Borczyskowski, "Discrimination of photoblinking and photobleaching on the single molecule level," *Journal of Luminescence*, vol. 127, no. 1, pp. 224–229, 2007.

[7] Isabel Rodrigues and J. Miguel Sanches, "Convex total variation denoising of poisson fluorescence confocal images with anisotropic filtering," *IEEE Transactions on Image Processing*, p. Accepted for publication, 2010.

[8] Paul Rodríguez and Brendt Wohlberg, "Efficient minimization method for a generalized total variation functional," *IEEE Transactions on Image Processing*, vol. 18, no. 2, pp. 322–332, Feb. 2009.

[9] A. Buades, B. Coll, and J. M. Morel, "A review of image denoising algorithms, with a new one," *SIAM Multiscale Model. Simul.*, vol. 4, no. 2, pp. 490–530, 2005.

[10] R.M. Willett and R.D. Nowak, "Fast multiresolution photon-limited image reconstruction," *Biomedical Imaging: Nano to Macro, 2004. IEEE International Symposium on*, pp. 1192–1195 Vol. 2, 15-18 April 2004.